

## Supporting Information

# **Layered Double Hydroxides Nanosheets: toward Ultrasensitive Tumor Microenvironment Responsive Synergetic Therapy**

Liang Yan,<sup>a‡</sup> Yingjie Wang,<sup>b‡</sup> Tingting Hu,<sup>a‡</sup> Xuan Mei,<sup>a</sup> Xiaojie Zhao,<sup>a</sup> Yanyan Bian,<sup>b</sup> Lan Jin,<sup>a</sup> Ruizheng Liang,<sup>\*a</sup> Xisheng Weng,<sup>\*b</sup> and Min Wei<sup>\*a</sup>

<sup>a</sup> State Key Laboratory of Chemical Resource Engineering, Beijing Advanced Innovation Center for Soft Matter Science and Engineering, Beijing University of Chemical Technology, Beijing 100029, P. R. China

<sup>b</sup> Department of Orthopaedics, Peking Union Medical College Hospital, Peking Union Medical College & Chinese Academy of Medical Sciences, Beijing 100730, P. R. China

E-mail: liangruizheng2000@163.com (R. Liang); xshweng@medmail.com.cn (X. Weng); weimin@mail.buct.edu.cn (M. Wei)

‡ These authors contributed equally to this work.

## Experimental Section

### 1. Preparation of materials.

**1.1 Materials.** All of the chemicals were of analytical-grade and obtained from commercial sources, which were used without any further purification. Manganese nitrate solution ( $\text{Mn}(\text{NO}_3)_2$ ), cobalt nitrate ( $\text{Co}(\text{NO}_3)_2 \cdot 6\text{H}_2\text{O}$ ), sodium nitrate ( $\text{NaNO}_3$ ), sodium hydroxide ( $\text{NaOH}$ ), formamide, 3-(4,5-dimethyl-2-thiazolyl)-2,5-diphenyl-2-H-tetrazolium bromide (MTT), 2,2,6,6-tetramethylpiperidine (TEMP) were purchased from Aladdin Chemical. Co. Ltd (Shanghai, China). Chlorin e6 (Ce6) was obtained from J&K Scientific (China). 2,7-Dichlorodihydrofluorescein diacetate (DCFH-DA), calceinacetoxymethyl ester (Calcein-AM), glutathione (GSH) and propidium iodide (PI) were purchased from Sigma-Aldrich Company (St. Louis, MO, USA). High glucose Dulbecco's modified Eagles medium (DMEM), 0.25% trypsin-EDTA and penicillin/streptomycin were obtained from Gibco (Invitrogen, Carlsbad, CA). Fetal bovine serum (FBS) was purchased from Excell Bio. Co., Ltd. (Shanghai, China). Hoechst 33342, phosphate-buffered saline (PBS), reduced glutathione (GSH) assay kit and Annexin V-FITC & propidium iodide apoptosis detection kit were purchased from Solarbio Science & Technology Co, Ltd (Beijing, China). Ultrapure water from a Milli-Q Millipore system was used in all the processes.

**1.2 Synthesis of CoMn-LDH ultrathin nanosheets.** CoMn-LDH nanosheets were prepared by a bottom-up method. Briefly, solution A:  $\text{Co}(\text{NO}_3)_2 \cdot 6\text{H}_2\text{O}$  (0.4 mmol) and  $\text{Mn}(\text{NO}_3)_2$  (0.2 mmol) were dissolved in deionized water (40 mL). Solution B:  $\text{NaNO}_3$  (0.2 mmol) was dissolved in deionized water containing 25% formamide (40 mL). Solution C:  $\text{NaOH}$  (0.15 mmol) was dissolved in deionized water (40 mL). Solution A and Solution C were slowly added to Solution B followed by stirring at room temperature for 1 h. After a thorough washing with deionized water and ethanol with centrifugation at 6000 rpm for three times, the resulting precipitate was redispersed in water and centrifuged at 2000 rpm to obtain CoMn-

LDH ultrathin nanosheets in the supernatant. Finally, a dialysis treatment (8 kDa) was carried out to remove residual formamide.

## 2. Materials properties.

**2.1 Drug loading.** Firstly, Ce6 was dissolved in dimethyl sulfoxide (DMSO), followed by adding into CoMn-LDH suspension with various mass ratios (from CoMn-LDH: Ce6=1:1 to CoMn-LDH: Ce6=1: 0.1) with stirring at room temperature for 12 h. The unloaded Ce6 and extra DMSO were removed by centrifugation at 10000 rpm for three times, and then the obtained Ce6/CoMn-LDH was re-dispersed in deionized water.

**2.2 The determination of loading content (LC).** The concentration of Ce6 in the initial drug solution and supernatant was measured by using a Shimadzu U-3000 spectrophotometer based on their absorbance at 405 nm. The LC of Ce6 was calculated according to the following equation:

$$LC=(W_{Fed}-W_{Non-encapsulated})/W_{LDH}\times 100\% \quad (1)$$

Where  $W_{Fed}$  is the initial mass of fed drug;  $W_{Non-encapsulated}$  is the drug mass in the supernatant after centrifugation, and  $W_{LDH}$  is the mass of CoMn-LDH added in the loading process.

**2.3 GSH-stimulated Ce6 release from Ce6/CoMn-LDH.** To determine the GSH-promoted Ce6 release, Ce6/CoMn-LDH ( $3 \mu\text{g mL}^{-1}$ ) was mixed with 0, 2, 4, 10 mM GSH, respectively. The released amount of Ce6 was measured according to the fluorescence emission spectroscopy.

**2.4 Detection of hydroxyl radical.** The determination of  $\bullet\text{OH}$  was based on the reaction between terephthalic acid (TA) and  $\bullet\text{OH}$ . TA itself has negligible fluorescence but is capable to capture  $\bullet\text{OH}$  and generate 2-hydroxy terephthalic acid with unique fluorescence at  $\sim 425$  nm. The fluorescence spectra were measured by a Hitachi F-7000 fluorescence spectrophotometer with an excitation wavelength of 315 nm and the slit width for excitation and emission is 2.5 nm.

**2.5 Detection of singlet oxygen production.** 1,3-diphenylisobenzofuran (DPBF) was used as a probe to detect singlet oxygen production. Briefly, A DPBF acetonitrile solution (10  $\mu\text{L}$ , 70  $\mu\text{M}$ ) was added into 1 mL of Ce6 and Ce6/CoMn-LDH (Ce6 equivalent concentration: 3  $\mu\text{g ml}^{-1}$ ) suspension with or without 10 mM of GSH, respectively. The mixed suspension was irradiated by a 650 nm laser (15  $\text{mW cm}^{-2}$ ) for 5 min and the UV-vis absorption spectra were monitored every minute. The singlet oxygen production efficiency is proportional to the decrease rate of DPBF absorption intensity at 410 nm.

**2.6 Detection of ROS by ESR.** Electron spin resonance (ESR) spectroscopy is used to identify the species of generated ROS. 2,2,6,6-tetramethylpiperidine (TEMP, 97  $\mu\text{M}$ ) as a  $^1\text{O}_2$  trapping agent was employed to examine the ESR signal of  $^1\text{O}_2$ . 5,5-Dimethyl-1-pyrroline N-oxide (DMPO) as the  $\bullet\text{OH}$  trapping agent was utilized to measure the ESR signal of  $\bullet\text{OH}$ .

**2.7 Measurement of  $\text{O}_2$  production.** For the measurement of  $\text{O}_2$  production ability of CoMn-LDH nanosheets, 50  $\mu\text{g mL}^{-1}$  of CoMn-LDH was added into an  $\text{H}_2\text{O}_2$  solution (100  $\mu\text{M}$ ). The oxygen concentration was recorded in real-time. The dissolved  $\text{O}_2$  was measured for 5 min with a portable dissolved oxygen meter.

**2.8 *In vitro* and *in vivo* self-enhanced MR imaging study.** The *in vitro* and *in vivo* self-enhanced MR imaging tests were performed on small animal MRI instruments in the field of 7.0 T (BioSpin, BRUKER, Germany). To test MRI performance of relaxation rate  $r_1$  and  $r_2$  *in vitro*, Mn concentration of CoMn-LDH was set to be 0, 0.031, 0.062, 0.125, 0.25, 0.5, 1 mM, respectively. The parameters of  $T_1$  RARE sequence used here were as follows: TR= 331.39 ms, TE= 5.48 ms, field of view= 35 mm $\times$ 35 mm, matrix size= 256 $\times$ 256, number of slices= 20, slice thickness= 1.0 mm, flip angle= 90 $^\circ$  and NEX= 5.  $T_2$ -weighted FR-FSE sequence: TR=3000 ms, TE=40 ms, field of view= 35 mm $\times$ 35 mm, matrix size= 256 $\times$ 256, number of slices= 20, slice thickness=1.0 mm, flip angle= 90 $^\circ$ . For *in vivo* MRI evaluation, CoMn-LDH was injected intravenously and monitored its tumor MRI performance at 0, 2, 4, 8, 12, 24 h

after injection.

### 3. *In vitro* studies.

**3.1 Cell line and culture.** U87mg, HepG2, 4T1 and Hela cells were incubated in a 25 cm<sup>2</sup> cell-culture flask and cultured well in DMEM containing 10% FBS and 1% penicillin-streptomycin (37 °C, 5% CO<sub>2</sub>). After cells spread over 80% of the bottom, trypsin (0.25%, 1.0 mL) was added to detach cells (2–3 min) followed by adding 2 mL of DMEM to terminate digestion.

**3.2 Cytotoxicity study.** To study the cytotoxicity of CoMn-LDH nanosheets, U87mg, HepG2, 4T1 and Hela cells (1×10<sup>4</sup> cells/well) were cultured into 96-well plates and incubated for 24 h (5% CO<sub>2</sub>; 37 °C), respectively, followed by addition of various concentrations of CoMn-LDH (10, 20, 50, 100 and 200 µg mL<sup>-1</sup>). After a further incubation of 24 h and thorough washing with PBS, the FBS-free medium containing 3-[4,5-dimethylthiazol-2-yl]-2,5-diphenyltetrazolium bromide (MTT) was added. The cell viability was determined by a Synergy 2 Multi-Mode Microplate Reader according to the absorbance at 490 nm.

The cell viability was calculated by the equation:

$$\text{Cell viability} = \frac{OD\ 490\ \text{nm}_{\text{the experimental group}}}{OD\ 490\ \text{nm}_{\text{the control group}}} \times 100\% \quad (2)$$

To further visualize the MTT results, Calcein-AM/PI was adopted to stain live and dead cells, respectively. Briefly, cells (2×10<sup>4</sup> cells/well) were seeded into 6-well plates and incubated for 24 h, followed by incubation with Ce6, Ce6/CoAl-LDH and Ce6/CoMn-LDH (Ce6: 3 µg mL<sup>-1</sup>, LDH: 30 µg mL<sup>-1</sup>, pH=6.5, 100 µM of H<sub>2</sub>O<sub>2</sub>) for 24 h, respectively. After irradiation with 650 nm laser (15 mW cm<sup>-2</sup>) for 30 min or not, the cells were stained with Calcein-AM (5 µg mL<sup>-1</sup>) and PI (10 µg mL<sup>-1</sup>). After culture for another 20 min and a thorough washing with PBS, the cells were monitored with a Leica confocal laser scanning microscopy.

**3.3 *In vitro* fluorescence image.** Hela cells were trypsinized and expanded in an incubator for 24 h (37 °C; 5% CO<sub>2</sub>) on confocal dishes (35 mm). Cells were then incubated with 2 mL of

Ce6 or Ce6/CoMn-LDH ( $3 \mu\text{g mL}^{-1}$ ) in complete DMEM for various incubation time (1, 4, 8, 12 and 24 h) in the dark. After the incubation, the cells were thoroughly washed with PBS for three times, and then Hoechst 33342 ( $10 \mu\text{g mL}^{-1}$ , 2 mL) was added to stain the nuclei. After 10 min, the cells were washed again with PBS for three times. Finally, images were obtained by using a confocal laser scanning microscope (Leica, Germany).

**3.4 Cellular ROS Detection.** HeLa cells were seeded into 6-well plates with a density of  $2 \times 10^5$  cells/well and incubated for 24 h. 2 mL of DCFH-DA ( $2 \times 10^{-5}$  M in FBS-free DMEM) was added and incubated for 30 min at  $37^\circ\text{C}$  in 5%  $\text{CO}_2$ . Then the culture media were replaced by media (acidulated DMEM with  $\text{pH} = 6.5$ ,  $100 \mu\text{M}$  of  $\text{H}_2\text{O}_2$ ) containing the following samples: Ce6, Ce6/CoAl-LDH and Ce6/CoMn-LDH (Ce6:  $3 \mu\text{g mL}^{-1}$ ). After incubation for another 8 h in 6-well plates and washing with PBS for three times, cells were exposed to 650 nm laser at a power of  $15 \text{ mW cm}^{-2}$  for 30 min. The cells were washed with PBS for three times, and the generated ROS inside the cells was measured by flow cytometer quantitatively and imaged by a Leica confocal laser scanning microscopy.

**3.5 *In vitro* CDT efficacy of CoMn-LDH.** HeLa cells at a density of  $1 \times 10^4$  cells per well were seeded and incubated in a 96-well plate for 24 h. To simulate the acidic extracellular microenvironment in solid tumor, DMEM ( $\text{pH} = 7.4$ ) was acidized to  $\text{pH} = 6.5$  by adding hydrochloric acid. The culture medium was then replaced by fresh medium ( $\text{pH} = 7.4$  and  $\text{pH} = 6.5$ ) with the introduction of  $\text{H}_2\text{O}_2$  ( $100 \mu\text{M}$ ) and various concentrations of CoMn-LDH or CoAl-LDH for 24 h. To investigate the effect of GSH on CDT performance, HeLa cells were firstly treated with  $2 \mu\text{M}$  of NMM for 20 min to regulate the level of GSH. After removing the culture medium, cells were incubated with various concentrations of CoAl-LDH at  $37^\circ\text{C}$  for 24 h. The culture media were replaced by FBS-free medium containing MTT. After 6 h of incubation, CDT efficacy was determined by measuring the absorbance at 490 nm.

**3.6 *In vitro* antitumor efficiency of Ce6/CoMn-LDH.** To study the antitumor performance

*in vitro*, HeLa cells were seeded into 96-well plates ( $1 \times 10^4$  cells/well) and incubated for 24 h. The culture medium was then replaced by fresh medium (pH = 6.5) containing  $\text{H}_2\text{O}_2$  (100  $\mu\text{M}$ ) and then treated with Ce6, Ce6/CoAl-LDH, Ce6/CoMn-LDH with various concentrations, respectively. After a further incubation of 8 h and thorough washing with PBS, the plates were irradiated with 650 nm laser ( $15 \text{ mW cm}^{-2}$ ) for 30 min and the cell viability was determined by colorimetric MTT. To further verify the MTT results, Calcein-AM/PI with Calcein-AM ( $5 \mu\text{g mL}^{-1}$ ) and PI ( $10 \mu\text{g mL}^{-1}$ ) were used to stain live and dead cells, respectively. The cells were monitored with an inverted fluorescence microscope.

**3.7 Combination Index (CI).** In a certain drug combination, CI is usually calculated to evaluate the synergetic effect of drugs. In this work, the synergistic effect in this CDT/PDT therapy was achieved through the combination of Ce6 and CoMn-LDH, so CI value was used to reveal the synergetic effect of CDT/PDT therapy compared with the sum of each treatment. CI is calculated by the following formula:

$$CI = D_1 / D_{m1} + D_2 / D_{m2} \quad (1)$$

where  $D_1$  and  $D_2$  are the concentrations of drug 1 and drug 2 that in combination to produce a certain amount of cell inhibition (*e.g.*, 50%); while  $D_{m1}$  and  $D_{m2}$  represent the concentrations of these drugs administered alone to induce the same cellular cytotoxicity. CI value significantly lower than 1.0 indicates synergism; CI value higher than 1.0 represents antagonism; CI value equal to 1.0 represents additivity.

#### **4. *In vivo* studies.**

**4.1 Animal experiments.** Male Balb/c mice (Balb/c-nude, ages 4–6 weeks) were purchased from Beijing Vital River Laboratory Animal Technology Co., Ltd and maintained in a 12 h/12 h light/dark cycle controlled environment. All animal studies were conducted under the guidelines of the National Institute of Health Guiding Principles for the Care and Use of Laboratory Animals, and the overall project protocols were approved by the Animal Care and

Use Committee of Peking Union Medical College Hospital. To establish the tumor models, mice were subcutaneously inoculated with  $1 \times 10^7$  Hela cells suspended in 100  $\mu\text{L}$  of PBS in the position of right-back. All the experiments were carried out when the tumor volume reached 70  $\text{mm}^3$ .

**4.2 *In vivo* fluorescence imaging.** The tumor-bearing mice were intravenously injected with PBS, Ce6 and Ce6/CoMn-LDH (200  $\mu\text{L}$ ; Ce6: 1  $\text{mg kg}^{-1}$ ; CoMn-LDH: 2  $\text{mg kg}^{-1}$ ), respectively. Fluorescence images at 0 h, 2 h, 4 h, 8h, 12 h and 24 h (excitation: 650 nm; emission: 710 nm) were obtained by an IVIS lumina fluorescence imaging system.

**4.3 Biodistribution analysis.** To study the biodistribution of Ce6/CoMn-LDH in balb/c mice, Ce6/CoMn-LDH (200  $\mu\text{L}$ ; Ce6: 1  $\text{mg kg}^{-1}$ ; CoMn-LDH: 2  $\text{mg kg}^{-1}$ ) suspension was *i.v.* injected into the tail vein. The mice were sacrificed after 4, 8, 12, 24 and 48 h post-administration. The fluorescence images of major organs were obtained on an IVIS lumina fluorescence imaging system. Tumors and organs are then weighed and digested with lysis buffer. Fluorescence intensity was measured by subtracting the background from untreated mice. The biodistribution was calculated and presented as a percentage of injected dose per gram of tissue (%ID  $\text{g}^{-1}$ ).

**4.4 *In vivo* antitumor therapy.** Mice were randomly divided into 6 groups (6 animals per group) and injected intravenously with different samples: Group 1: PBS (200  $\mu\text{L}$ ); Group 2: Ce6 (200  $\mu\text{L}$ ;  $\text{mg kg}^{-1}$ ); Group 3: Ce6 (200  $\mu\text{L}$ ; 1  $\text{mg kg}^{-1}$ ) with irradiation; Group 4: CoMn-LDH (200  $\mu\text{L}$ ; 10  $\text{mg kg}^{-1}$ ); Group 5: Ce6/CoMn-LDH (200  $\mu\text{L}$ ; Ce6: 1  $\text{mg kg}^{-1}$ ; CoMn-LDH: 10  $\text{mg kg}^{-1}$ ); Group 6: Ce6/CoMn-LDH (200  $\mu\text{L}$ ; Ce6: 1  $\text{mg kg}^{-1}$ ; CoMn-LDH: 10  $\text{mg kg}^{-1}$ ) with irradiation. The irradiation was carried out for 30 min (15  $\text{mW cm}^{-2}$ ). The tumor size was measured with the vernier caliper every two days with 14 days' treatment, and the volume was calculated as:

$$\text{Volume} = \text{tumor length} \times \text{tumor width}^2 \times 0.5 \quad (3)$$

Relative tumor volume was calculated as  $V/V_0$ , in which  $V$  and  $V_0$  are the tumor volume at the measured and initial time, respectively.

**4.5 Histology examination.** After two weeks of treatment, the mice were euthanized. Tumors and main organs were fixed in 4% formalin for histology analysis. And then the tissues were sliced to 3–5 mm for hematoxylin and eosin (H&E) staining and imaging.

**4.6 *In vivo* toxicity study.** The mice were randomly divided into two groups including blank group and Ce6/CoMn-LDH treated group. For the Ce6/CoMn-LDH treated group, mice were *i.v.* injected with 200  $\mu\text{L}$  of Ce6/CoMn-LDH (Ce6: 1  $\text{mg kg}^{-1}$ ; CoMn-LDH: 10  $\text{mg kg}^{-1}$ ), and then the blood was collected for subsequent analysis after post-injection for 1 day and 7 days. The blood cell counts were measured on an automated hematology analyzer (Bayer Advia 2120). The serum biochemistry parameters including blood urea nitrogen (BUN), creatinine (CR), aspartate aminotransferase (AST) and alanine aminotransferase (ALT) were tested using the automatic biochemical analyzer (Olympus AU400).

**5. Instrumentation and Characterization.** The morphology of CoMn-LDH and Ce6/CoMn-LDH was investigated on a high-resolution transmission electron microscope (HRTEM, JEOL, JEM-2100, 200 kV). The thickness of the CoMn-LDH nanosheets was recorded in a tapping mode using an atomic force microscope (AFM, Veeco, NanoScope IIIa). X-ray diffraction (XRD) patterns of CoMn-LDH and bulk CoMn-LDH were studied using a Shimadzu, XRD-6000 diffractometer, ranging from  $3^\circ$  to  $70^\circ$  at  $0.04^\circ/\text{s}$  in the scanning step (reflection mode,  $\text{CuK}\alpha$  radiation  $\lambda = 0.154056 \text{ nm}$ , at 40 kV). XPS spectra were studied by PHIQ2000 X-ray photoelectron spectroscopy. Zeta potential and dynamic light scattering (DLS) diameter of CoMn-LDH and Ce6/CoMn-LDH were measured on a photon correlation spectrum (PCS, Nanosizer Nano ZS, MALVERN Instruments). Fourier transform infrared (FT-IR) spectroscopy was performed on a Nicolet 605 XB FT-IR spectrometer from  $400 \text{ cm}^{-1}$  to  $4000 \text{ cm}^{-1}$  with a resolution of  $2 \text{ cm}^{-1}$ . The UV-vis absorption spectra were recorded by using a

Shimadzu U-3000 spectrophotometer with a slit width of 1 nm in the range 200–900 nm.

**6. Statistical analysis.** Data were expressed as mean  $\pm$  standard deviation (s.d.). Statistical comparisons were made by unpaired Student's t-test (between two groups) and one-way ANOVA (for multiple comparisons) followed by Tukey's post-test:  $*p < 0.05$ .

**7. Computational details.** All calculations were used with the CASTEP code in the Materials Studio 6.1 software package (Accelrys Software Inc., San Diego, CA).<sup>[1]</sup> The Perdew-Burke-Ernzerh (PBE) functional of generalized gradient approximation (GGA) was used as the exchange-correlation functional of the electrons.<sup>[2]</sup> The Broyden-Fletcher-Goldfarb-Shanno (BFGS) algorithm was used to search for the potential energy surface.<sup>[3]</sup> The Tkatchenko-Scheffler method was used to describe the noncovalent forces.<sup>[4]</sup> The cutoff energy was set to be 260 eV. CoMn-LDH was constructed with symmetry  $P\bar{3}M1$ , with the corresponding lattice parameters:  $a=b=3.02 \text{ \AA}$ ,  $c=8.55 \text{ \AA}$ . The supercell of the model was  $3 \times 3 \times 1$  in the  $a$ ,  $b$ ,  $c$  direction. The molar ratio of Co to Mn was 2:1. During the calculations, the convergence tolerance was set as follows: energy =  $5.0e^{-5}$  eV/atom; maximum force =  $0.1 \text{ eV / \AA}$ ; maximum displacement =  $0.005 \text{ \AA}$ .

Adsorption energy ( $E_{\text{ads}}$ ) was calculated by the equation:

$$E_{\text{ads}} = E_{\text{R}^*} - (E_{\text{R}} + E_*) \quad (4)$$

where  $E_{\text{R}}$  is the energy of reactants;  $E_*$  is the energy of the surface, and  $E_{\text{R}^*}$  is the system energy after surface adsorption.

## Supplementary Figures

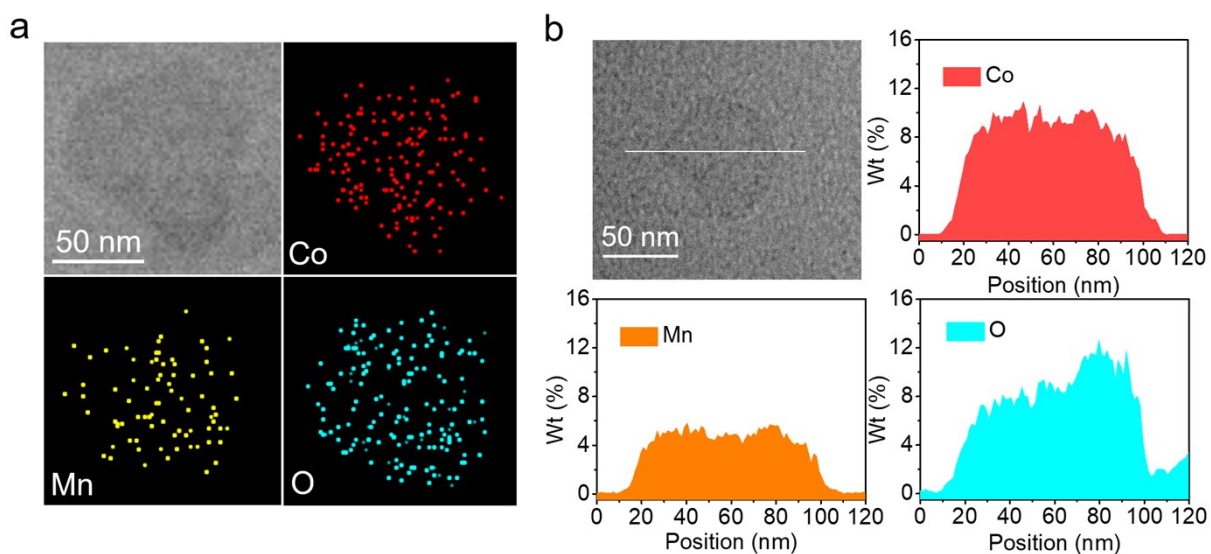


**Figure S1.** (a) STEM image of CoMn-LDH nanosheets with corresponding EDX mapping images for Co, Mn and O, respectively. (b) Elemental EDX line profiles of Co, Mn and O, respectively.

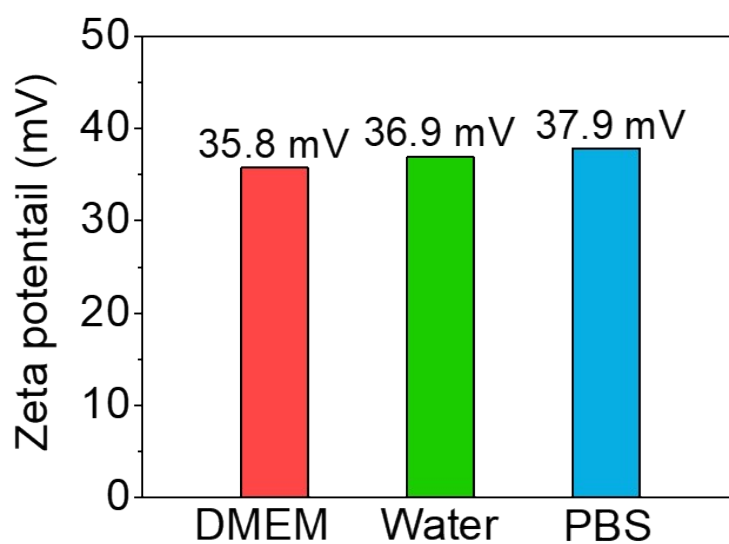


**Figure S2.** Surface Zeta potential of CoMn-LDH nanosheets in DMEM, and PBS solution, respectively.

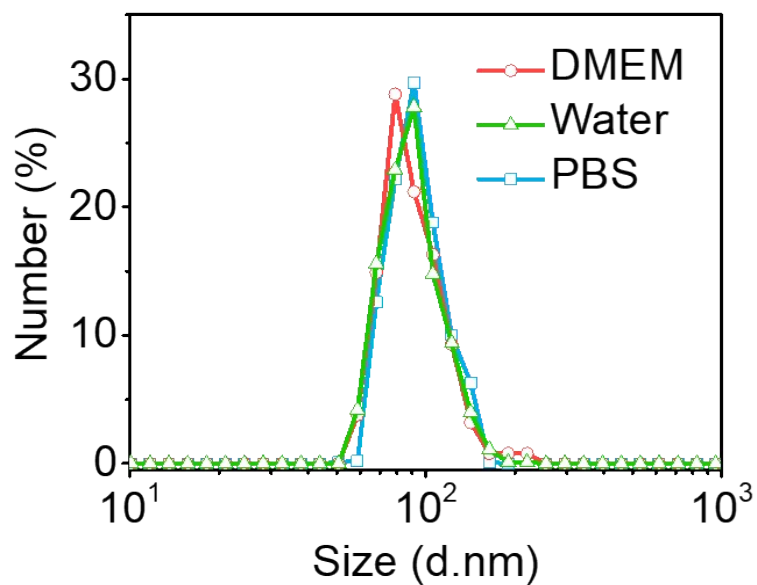


**Figure S3.** Size distribution of CoMn-LDH nanosheets in PBS, water and DMEM culture medium, respectively.

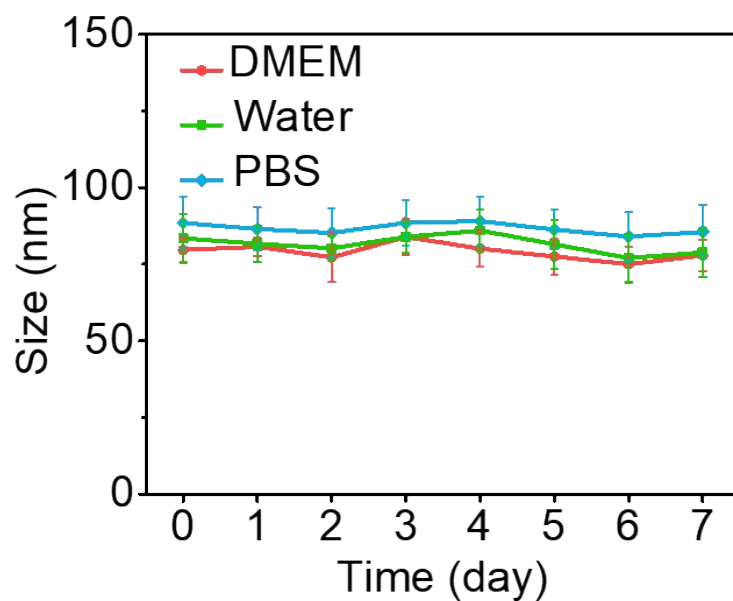


**Figure S4.** Stability tests of Ce6/CoMn-LDH in PBS, water and DMEM by monitoring particle size for 7 days. Error bars stand for  $\pm$  s.d. ( $n = 3$ ).



**Figure S5.** Photograph of CoMn-LDH suspension before (left) and after (right) adding GSH.

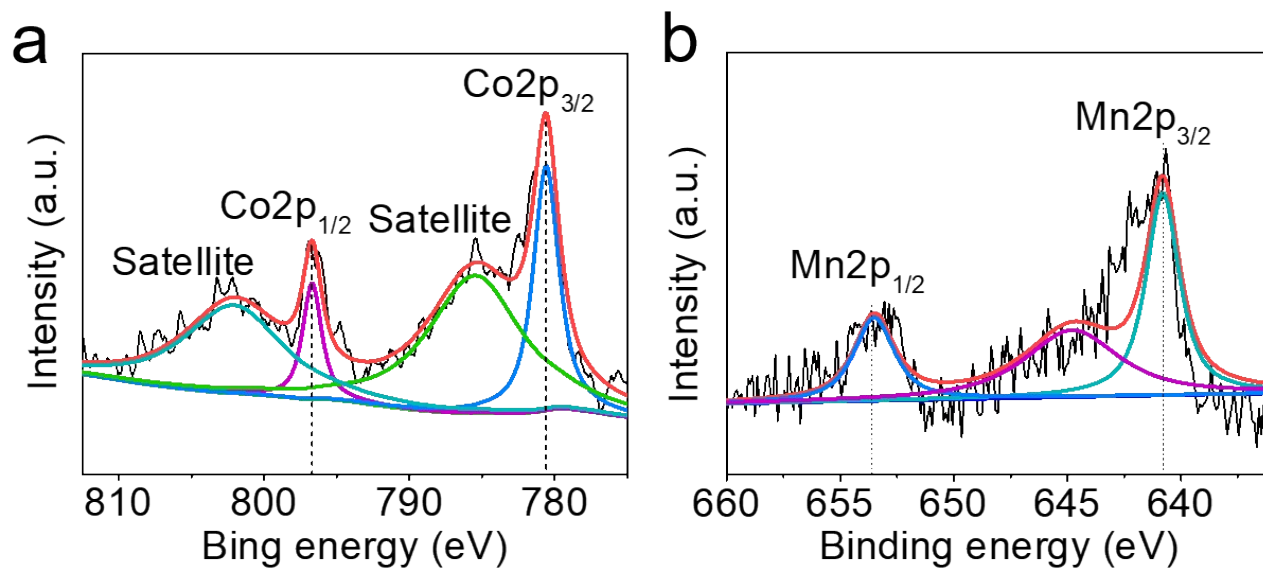


**Figure S6.** XPS spectra of (a) Co  $2p$  and (b) Mn  $2p$  for CoMn-LDH after GSH treatment.

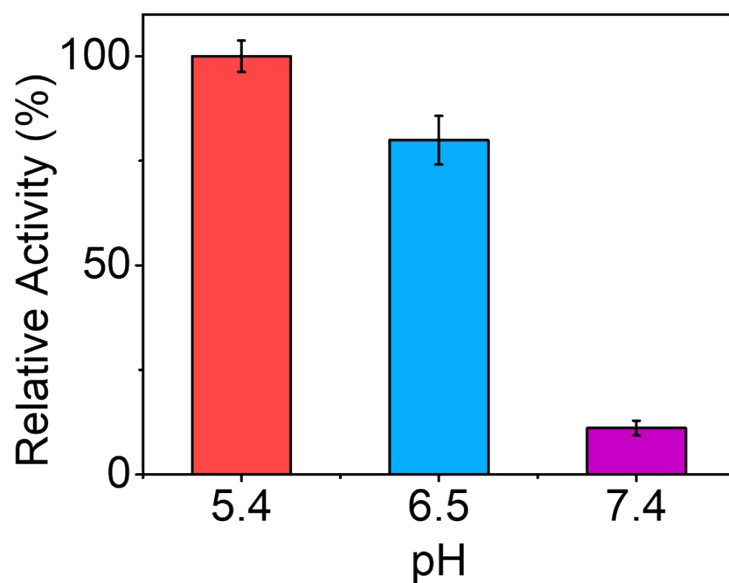


**Figure S7.** Influence of pH value on the CDT ability of CoMn-LDH. Error bars stand for  $\pm$  s.d. ( $n = 3$ ).

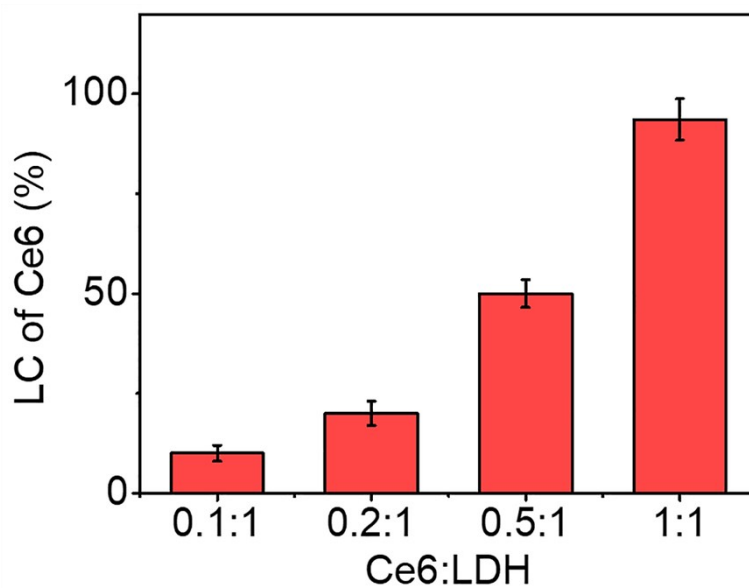


**Figure S8.** LC of Ce6 onto CoMn-LDH nanosheets with various mass ratios. Error bars stand for  $\pm$  s.d. ( $n = 3$ ).

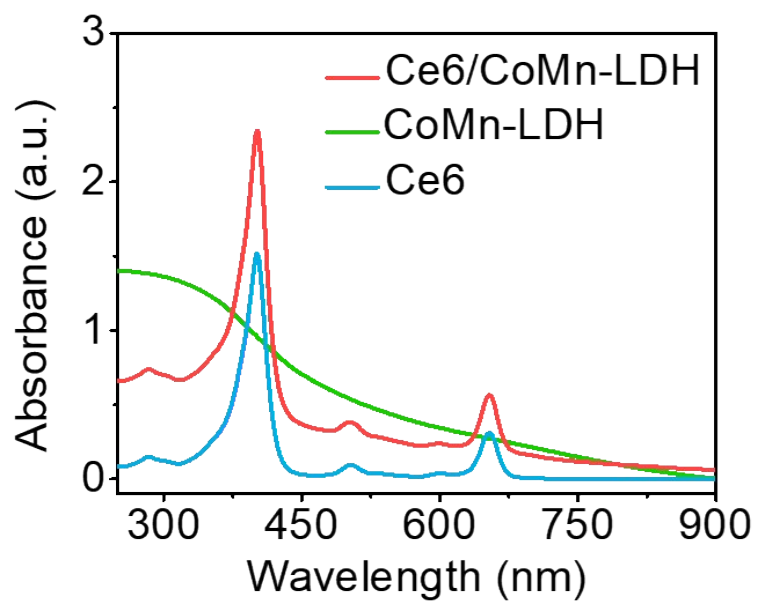


**Figure S9.** UV-vis-NIR spectra of Ce6, CoMn-LDH and Ce6/CoMn-LDH, respectively.

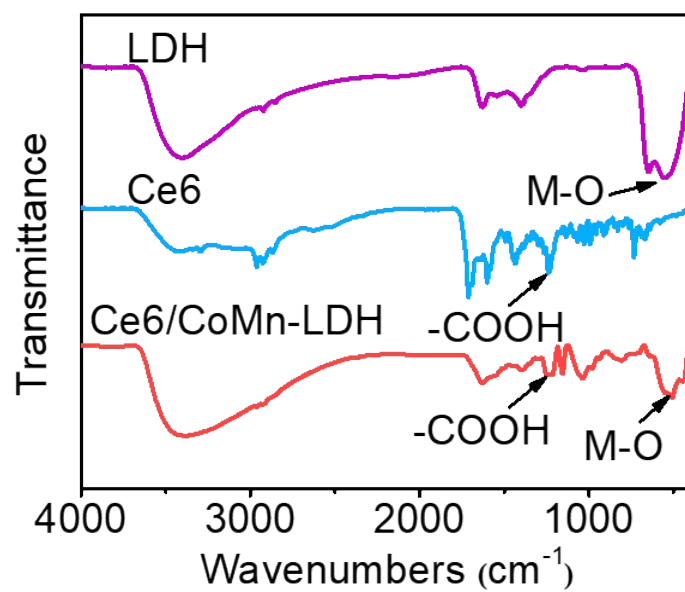


**Figure S10.** FT-IR spectra of CoMn-LDH, Ce6 and Ce6/CoMn-LDH, respectively.

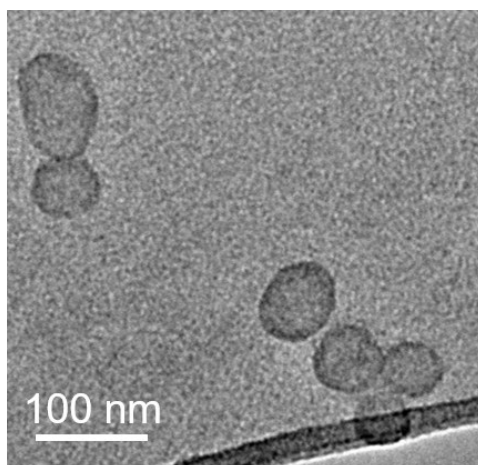


**Figure S11.** HRTEM image of the Ce6/CoMn-LDH sample.

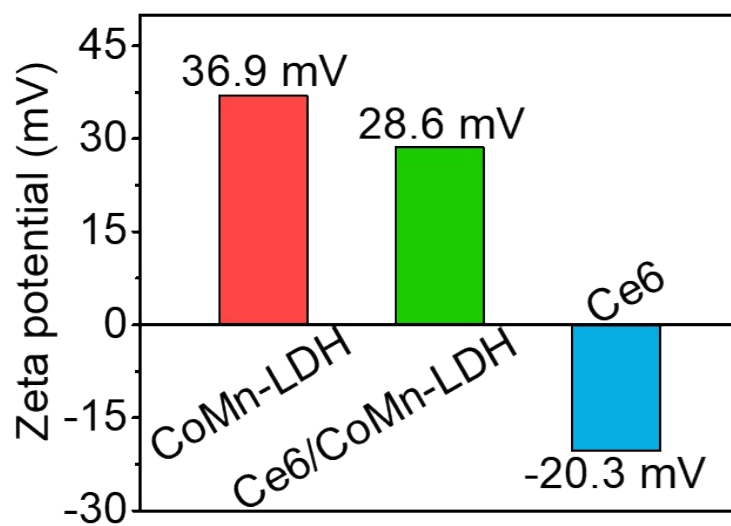


**Figure S12.** Surface zeta potential of CoMn-LDH, Ce6/CoMn-LDH and Ce6, respectively.

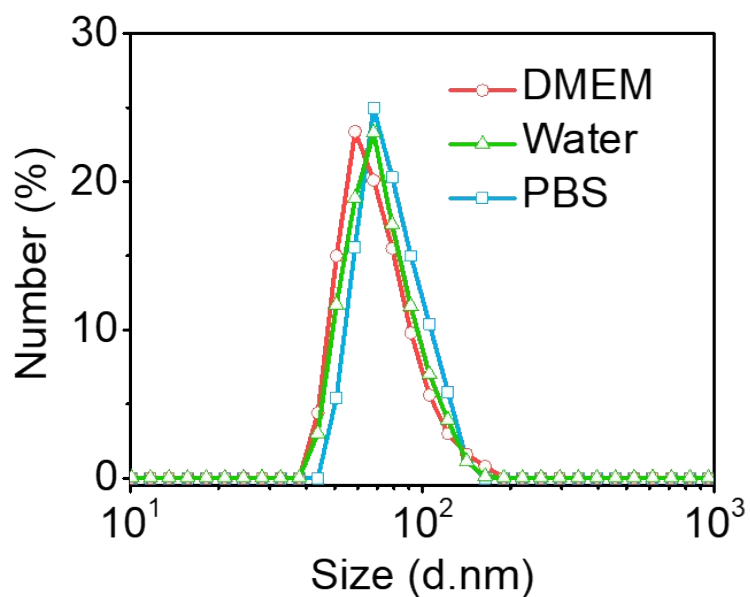


**Figure S13.** Size distribution of Ce6/CoMn-LDH in water, PBS and DMEM culture medium, respectively.

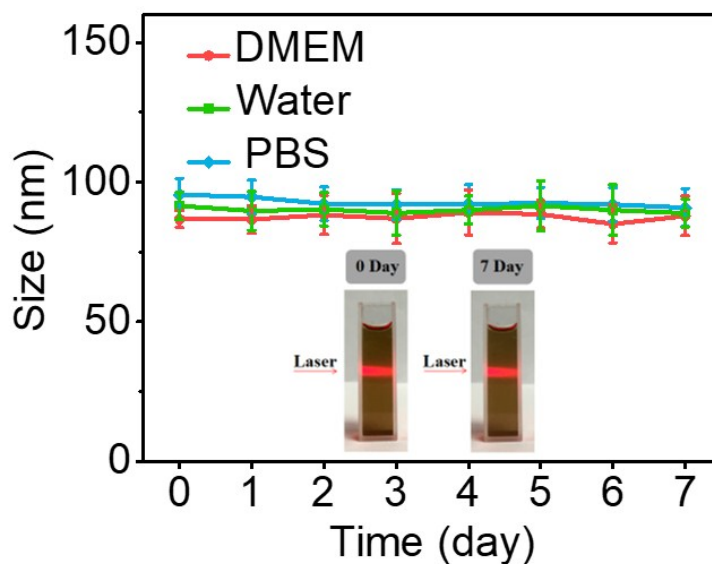


**Figure S14.** Stability tests of Ce6/CoMn-LDH in water, PBS and DMEM by monitoring particle size for 7 days. The inset photographs show the Tyndall effect of Ce6/CoMn-LDH in aqueous solution at day 1 and day 7, indicating a good dispersibility and stability. Error bars stand for  $\pm$  s.d. ( $n = 3$ ).

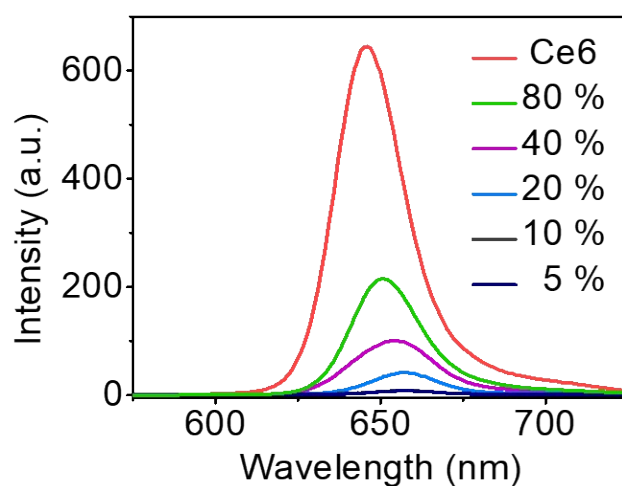


**Figure S15.** Fluorescence spectra of Ce6 and Ce6/CoMn-LDH with various mass ratios.

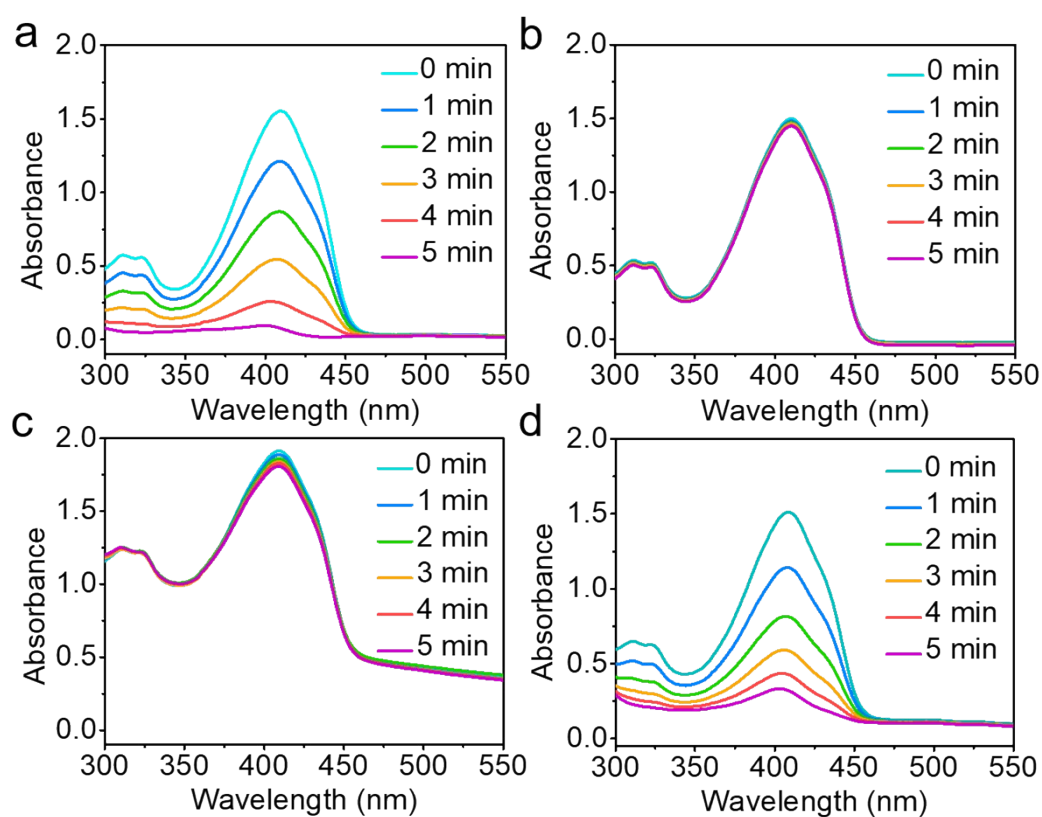


**Figure S16.** Photodynamic performance of different samples. Decay curves of DPBF absorbance in the presence of (a) Ce6 without GSH, (b) Ce6 with GSH, (c) Ce6/CoMn-LDH without GSH, (d) Ce6/CoMn-LDH with GSH as a function of irradiation time (650 nm, 15  $\text{mW cm}^{-2}$ ).

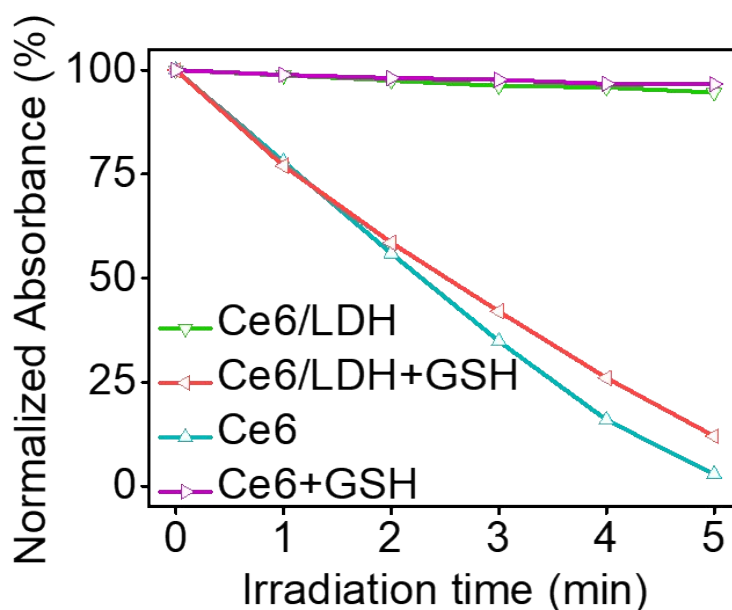


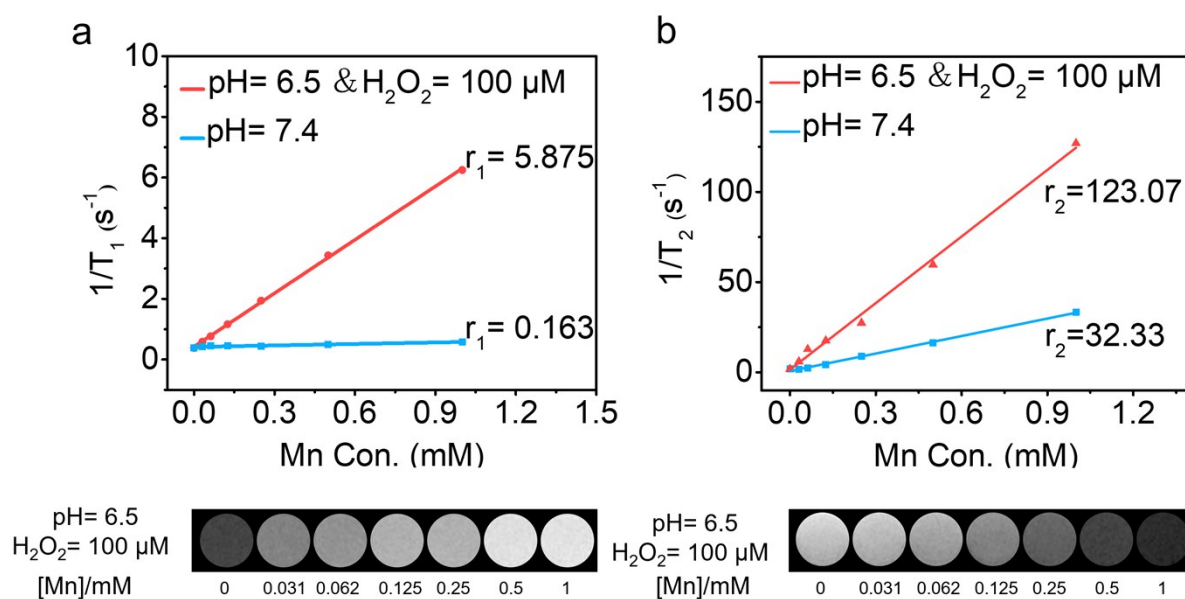
**Figure S17.** Normalized absorbance of DPBF in the presence of Ce6, Ce6/CoMn-LDH, Ce6 with GSH (10 mM), Ce6/CoMn-LDH with GSH (10 mM), upon 650 nm irradiation (15 mW cm<sup>-2</sup>).

**Table S1.** Calculated Energies of GSH Adsorbed on Various Sites (Top, Bridge, Fcc and Hollow) of CoMn-LDH or MnO<sub>2</sub>.

	Adsorption site	E/eV	Eads/eV
Co <sub>2</sub> Mn <sub>1</sub> -NO <sub>3</sub> -LDH(003)+ GSH	Top	-57108.28507	-3.128900653
	Bridge	-57107.7998	-2.643631513
	Fcc	-57107.92021	-2.764035383
MnO <sub>2</sub> (003)+ GSH	Top	-29915.64926	-1.182583063
	Bridge	-29915.41854	-0.951863633
	Hollow	-29915.4885	-1.021819843

**Table S2.** Mn–O distance of CoMn-LDH and the average Mn–O distance.

Bond length of Mn–O /Å						Average length
2.0842	2.10739	2.14489	2.06941	2.09429	2.12134	
2.08887	2.11061	2.16228	2.07551	2.09805	2.1315	2.1110439
2.09312	2.11963	2.18062	2.07875	2.10233	2.1360	

**Figure S18.** (a) T<sub>1</sub>-weighted relaxivity and T<sub>1</sub>-weighted MR images vs. Mn concentration for CoMn-LDH monolayer treated with 100 μM of H<sub>2</sub>O<sub>2</sub> at pH= 6.5. (b) T<sub>2</sub>-weighted relaxivity and T<sub>2</sub>-weighted MR images vs. Mn concentration for CoMn-LDH monolayer treated with 100 μM of H<sub>2</sub>O<sub>2</sub> at pH= 6.5.

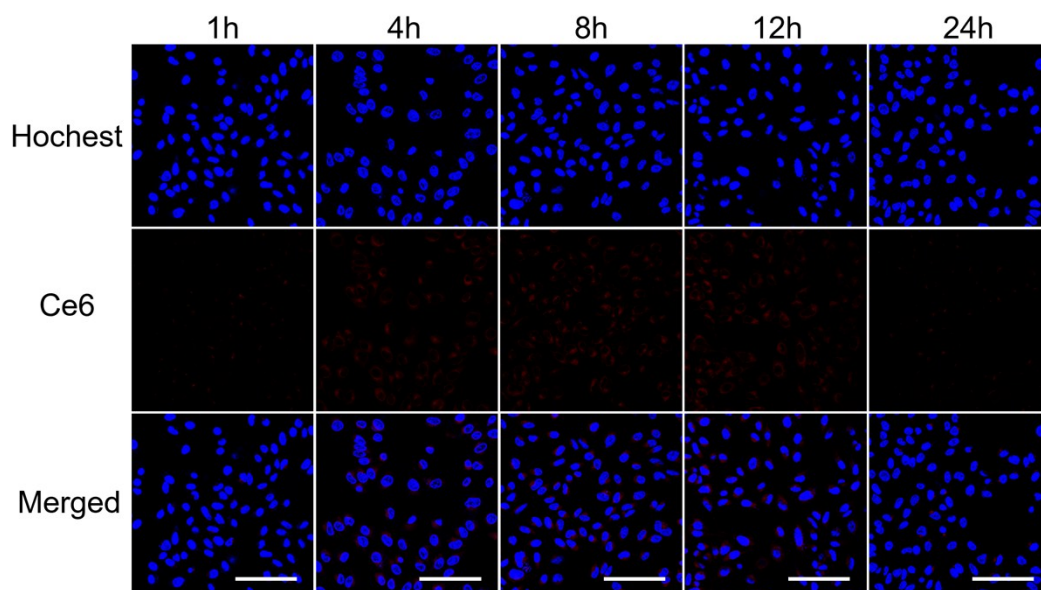


**Figure S19.** Fluorescence images of HeLa cells treated with Ce6 at various time points. Blue and red represent Hoechst and Ce6 fluorescence, respectively. Scale bar, 100  $\mu$ m.

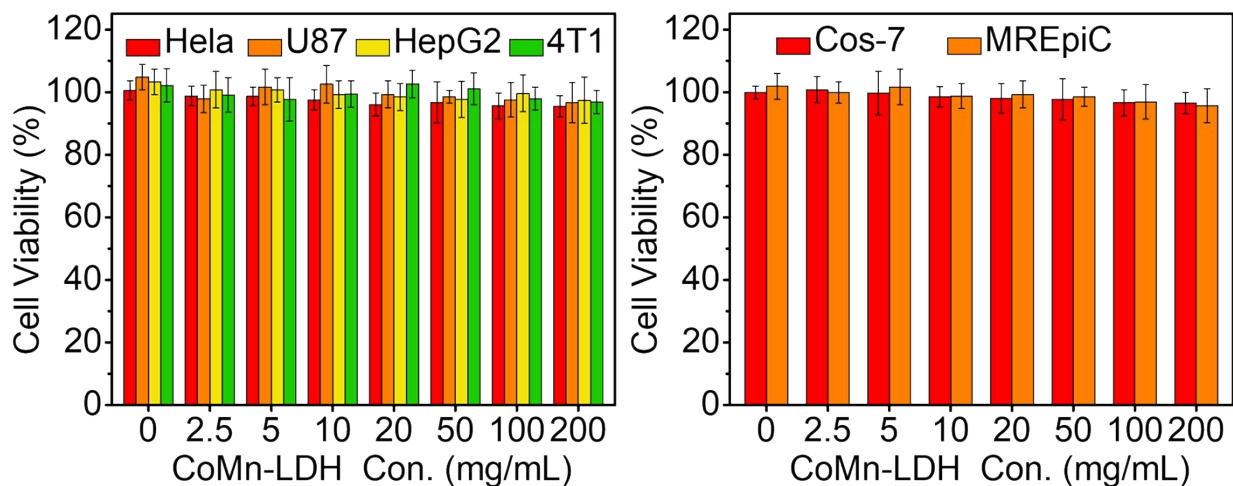


**Figure S20.** Cell viability of cancer cells (Hela, U87mg, HepG2 and 4T1) and normal cells (Cos-7 and MREpiC) incubated with various concentrations of CoMn-LDH nanosheets. Error bars stand for  $\pm$  s.d. ( $n = 3$ ).

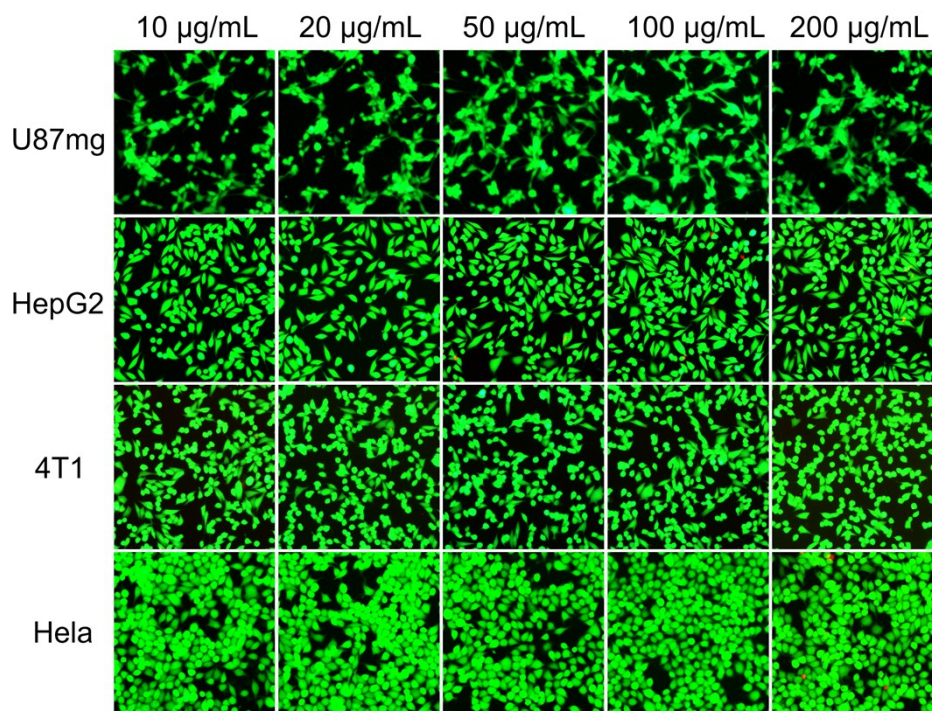


**Figure S21.** Calcein-AM/PI staining of U87mg, HepG2, 4T1 and HeLa cells incubated with various concentrations of CoMn-LDH nanosheets.

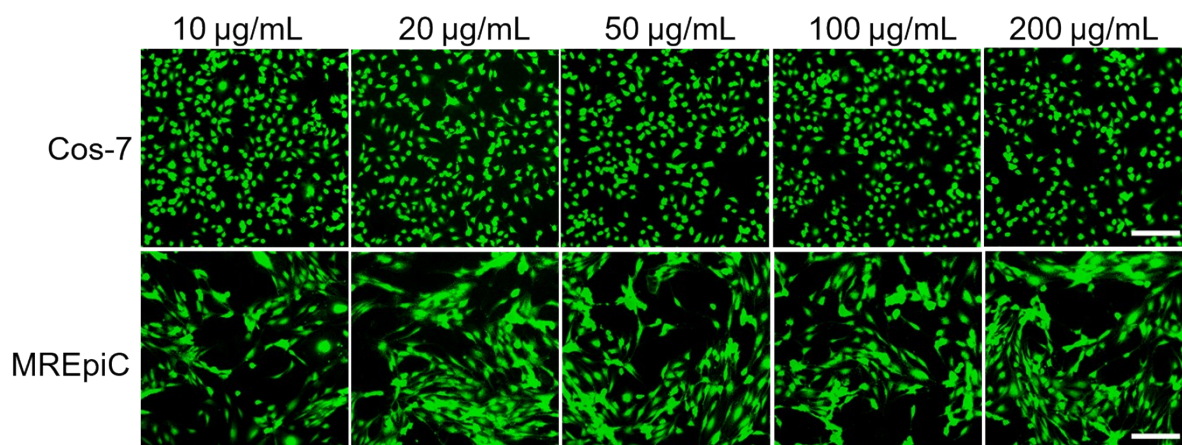


**Figure S22.** Calcein-AM/PI staining of Cos-7 and MREpiC cells incubated with various concentrations of CoMn-LDH nanosheets. Scale bar, 100  $\mu\text{m}$ .

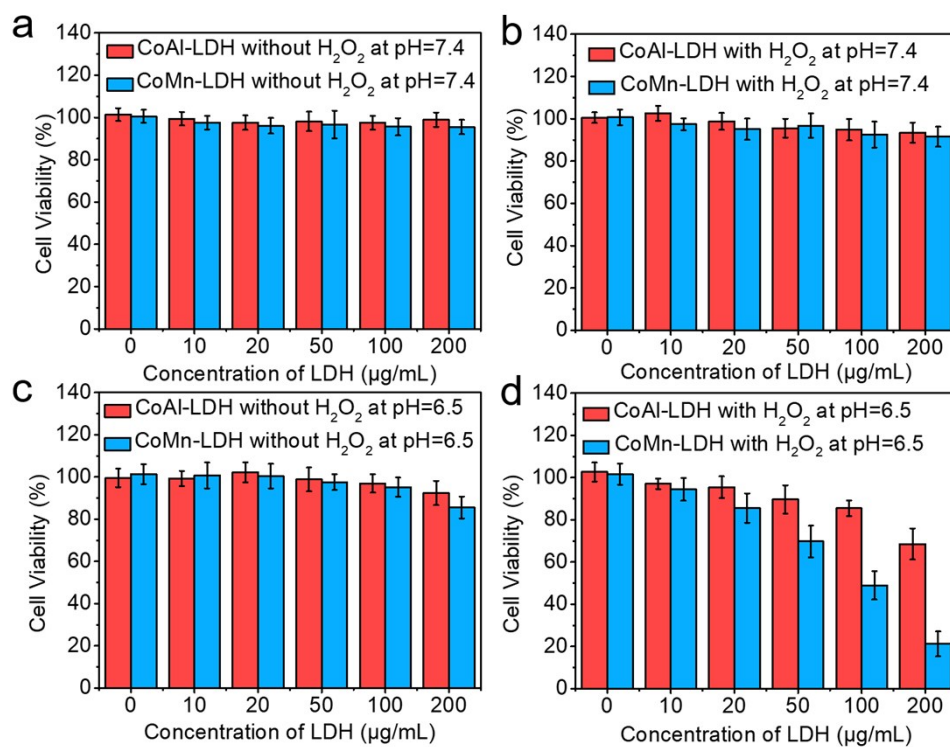


**Figure S23.** Viability of HeLa cells treated with CoAl-LDH or CoMn-LDH at pH=7.4: (a) without H<sub>2</sub>O<sub>2</sub>, (b) in the presence of H<sub>2</sub>O<sub>2</sub> (100 µM). Viability of HeLa cells treated with CoAl-LDH or CoMn-LDH on at pH=6.5: (c) without H<sub>2</sub>O<sub>2</sub>, (d) in the presence of H<sub>2</sub>O<sub>2</sub> (100 µM). Error bars stand for ± s.d. ( $n = 3$ ).

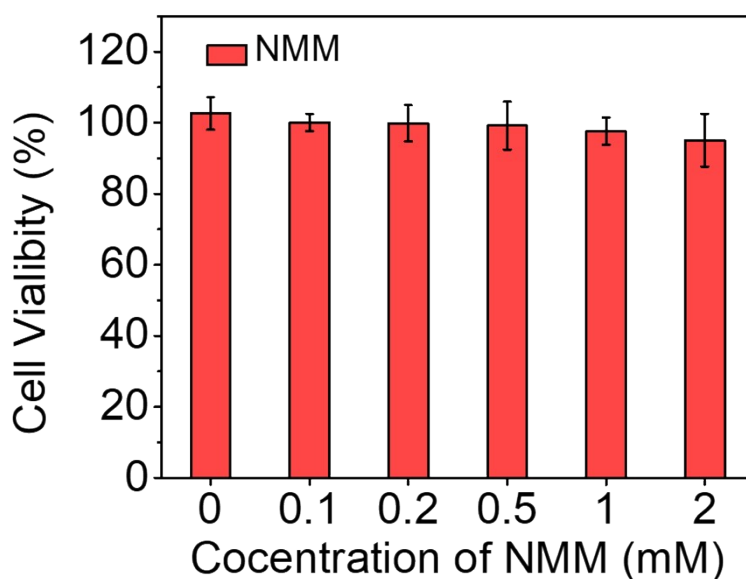


**Figure S24.** Viability of HeLa cells treated with various concentrations of NMM. Error bars stand for ± s.d. ( $n = 3$ ).

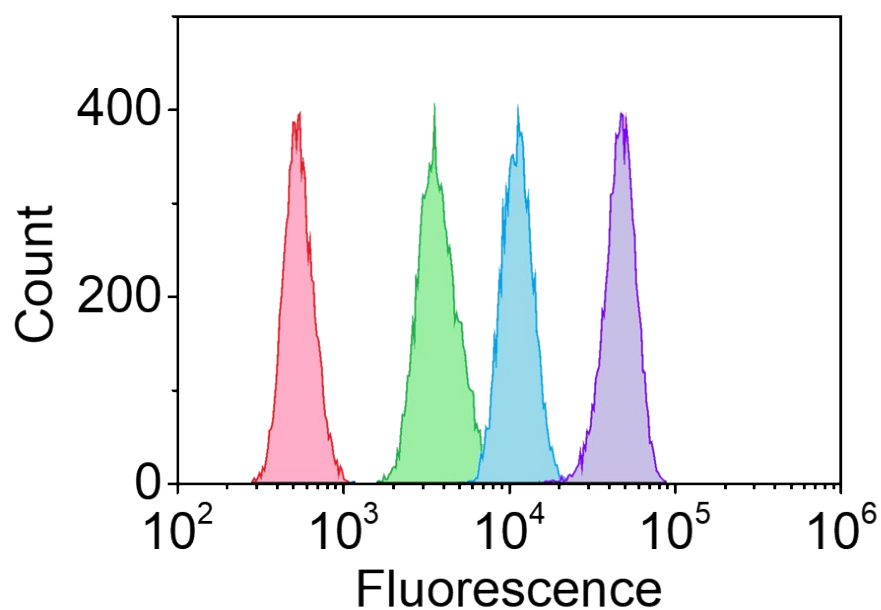


**Figure S25.** Flow cytometry measurements of DCFH-DA signal for PBS (pink), Ce6 (green), Ce6/CoAl-LDH (blue) and Ce6/CoMn-LDH (purple), respectively.

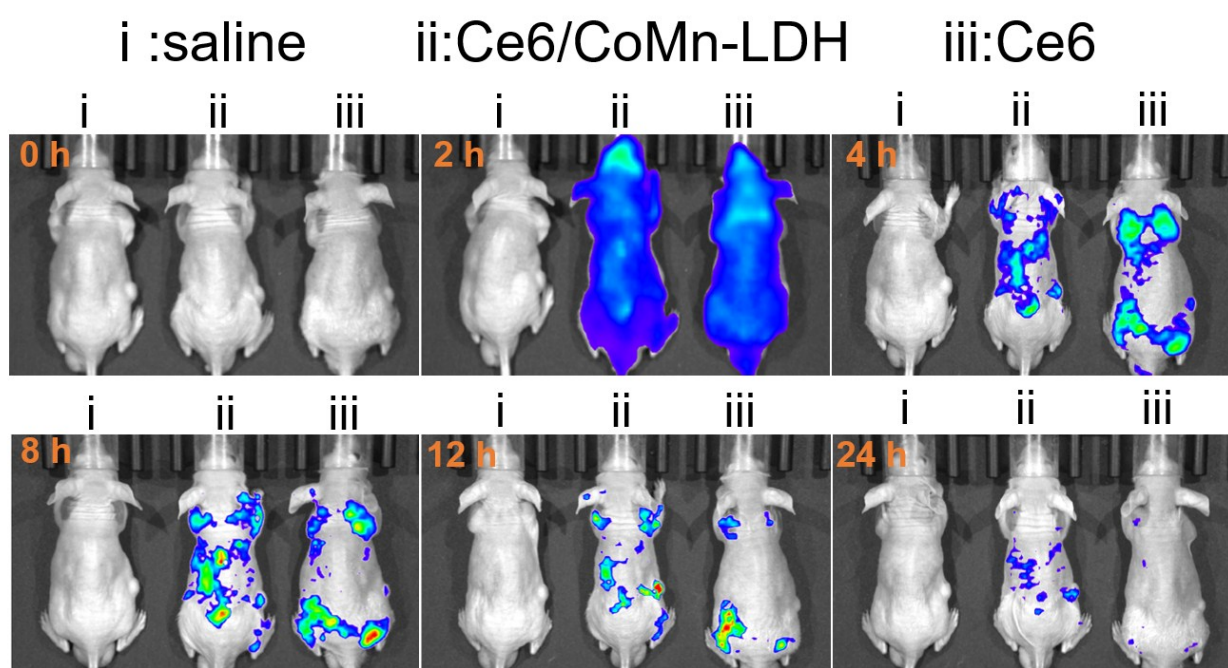


**Figure S26.** *In vivo* fluorescence imaging of nude mice bearing HeLa tumors at different time points after intravenous injection of saline, Ce6/CoMn-LDH and Ce6, respectively.

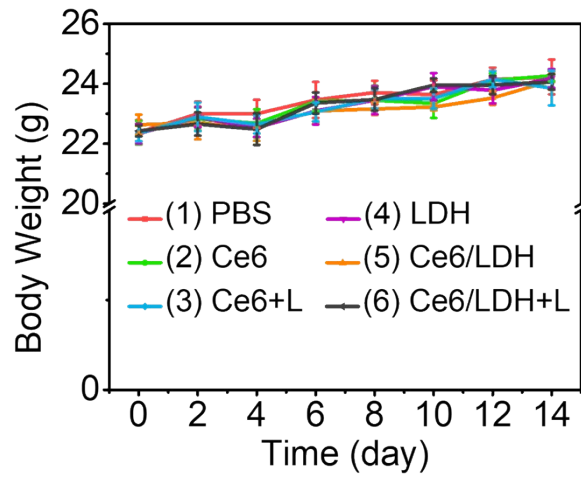


**Figure S27.** Bodyweight changes of HeLa tumor-bearing mice after various treatments. Error bars stand for  $\pm$  s.d. ( $n = 6$ ).

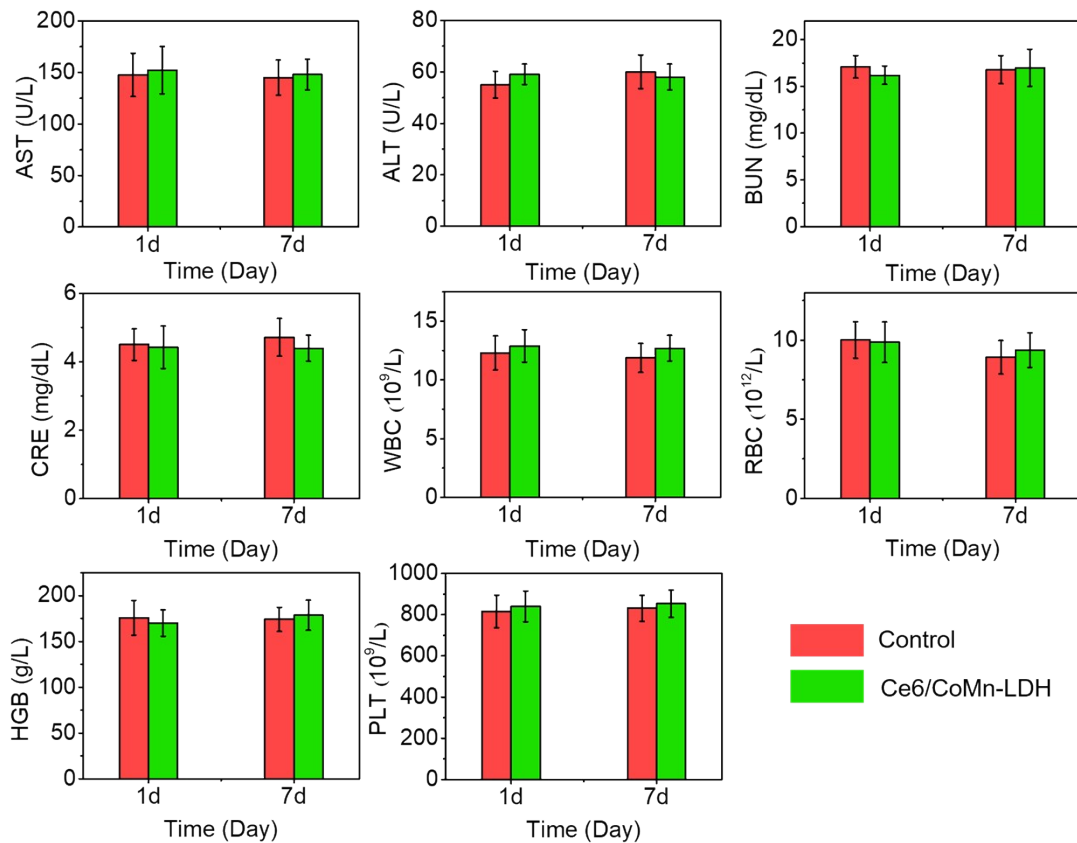


**Figure S28.** *In vivo* biosafety of Ce6/CoMn-LDH: the nude mice bearing HeLa tumors after injection of saline (control) and Ce6/CoMn-LDH for 1 day and 7 days. The blood cell counts, kidney and liver function markers including BUN, CR, ALT and AST were detected. Error bars stand for  $\pm$  s.d. ( $n = 3$ ).

## Reference

- [1] M. D. Segall, P. Lindan, M. J. Probert, C. J. Pickard, P. J. Hasnip, S. J. Clark and M. C. Payne, *J. Phys.: Condens. Matter*, 2002, **14**, 2717–2744.
- [2] J. P. Perdew, K. Burke and M. Ernzerhof, *Phys. Rev. Lett.*, 1996, **77**, 3865.
- [3] J. M. Anglada and J. M. Bofill, *J. Comput. Chem.*, 1998, **19**, 349–362.
- [4] A. Tkatchenko and M. Scheffler, *Phys. Rev. Lett.*, 2009, **102**, 073005.